Whole Body UVA Irradiation Lowers Systemic Blood Pressure by Release of Nitric Oxide From Intracutaneous Photolabile Nitric Oxide Derivates

Christian Opländer, Christine M. Volkmar, Adnana Paunel-Görgülü, Ernst E. van Faassen, Christian Heiss, Malte Kelm, Daniel Halmer, Manfred Mürtz, Norbert Pallua and Christoph V. Suschek

Circ Res. 2009;105:1031-1040; originally published online September 24, 2009;
doi: 10.1161/CIRCRESAHA.109.207019
Circulation Research is published by the American Heart Association, 7272 Greenville Avenue, Dallas, TX 75231

Print ISSN: 0009-7330. Online ISSN: 1524-4571

Whole Body UVA Irradiation Lowers Systemic Blood Pressure by Release of Nitric Oxide From Intracutaneous Photolabile Nitric Oxide Derivates

Christian Opländer, Christine M. Volkmar, Adnana Paunel-Görgülü, Ernst E. van Faassen, Christian Heiss, Malte Kelm, Daniel Halmer, Manfred Mürtz, Norbert Pallua, Christoph V. Suschek

Rationale: Human skin contains photolabile nitric oxide derivates like nitrite and *S*-nitroso thiols, which after UVA irradiation, decompose and lead to the formation of vasoactive NO.

Objective: Here, we investigated whether whole body UVA irradiation influences the blood pressure of healthy volunteers because of cutaneous nonenzymatic NO formation.

Methods and Results: As detected by chemoluminescence detection or by electron paramagnetic resonance spectroscopy in vitro with human skin specimens, UVA illumination (25 J/cm^2) significantly increased the intradermal levels of free NO. In addition, UVA enhanced dermal *S*-nitrosothiols 2.3-fold, and the subfraction of dermal *S*-nitrosoalbumin 2.9-fold. In vivo, in healthy volunteers creamed with a skin cream containing isotopically labeled ^{15}N-nitrite, whole body UVA irradiation (20 J/cm^2) induced significant levels of ^{15}N-labeled *S*-nitrosothiols in the blood plasma of light exposed subjects, as detected by cavity leak out spectroscopy. Furthermore, whole body UVA irradiation caused a rapid, significant decrease, lasting up to 60 minutes, in systolic and diastolic blood pressure of healthy volunteers by 11±2% at 30 minutes after UVA exposure. The decrease in blood pressure strongly correlated (R^2=0.74) with enhanced plasma concentration of nitrosated species, as detected by a chemiluminescence assay, with increased forearm blood flow (+26±7%), with increased flow mediated vasodilation of the brachial artery (+68±22%), and with decreased forearm vascular resistance (−28±7%).

Conclusions: UVA irradiation of human skin caused a significant drop in blood pressure even at moderate UVA doses. The effects were attributed to UVA induced release of NO from cutaneous photolabile NO derivates. (*Circ Res*. 2009;105:1031-1040.)

Key Words: nitric oxide ■ nitrite ■ nitroso compounds ■ UVA ■ decomposition ■ photolysis ■ human skin

Apart from its effects on stroke, renal failure, and peripheral arterial disease, systemic arterial hypertension is a major risk factor for cardiovascular complications, including coronary artery disease, heart failure and sudden cardiac death.[1,2]

Interestingly, mean systolic and diastolic pressures and the prevalence of hypertension vary throughout the world. Many data suggest a linear rise in blood pressure at increasing distances from the equator. Similarly, blood pressure is higher in winter than summer.[3] Previously, it has been hypothesized that reduced epidermal vitamin D_3 photosynthesis associated with decreased UV light intensity at distances from the equator, alone or when coupled with decreased dietary calcium and vitamin D, may be associated with reduced vitamin D stores and increased parathyroid hormone secretion.[4] These changes may stimulate growth of vascular smooth muscle and enhance its contractility by affecting intracellular calcium, adrenergic responsiveness, and/or endothelial function. Thus, UV light intensity and efficiency of epidermal vitamin D_3 photosynthesis may contribute to geographic and racial variability in blood pressure and the prevalence of hypertension.[4]

However, there might exist another or additional supporting mechanism, respectively, by which ambient electromagnetic radiation may affect blood pressure. Furchgott et al noted as long ago as 1961 that exposure to sun light relaxed isolated arterial preparations,[5] although other types of smooth muscle tissue were much less sensitive.[6] The vascular photorelaxation was wavelength-dependent, increasing as wavelength was reduced from the visible into the UV range, and it

Original received August 10, 2009; revision received September 13, 2009; accepted September 16, 2009.

From the Department of Plastic and Reconstructive Surgery, Hand Surgery, and Burn Center (C.O., C.M.V., N.P., C.V.S.), Medical Faculty, RWTH Aachen University, Germany; Department of Trauma and Hand Surgery (A.P.-G.), University Hospital Düsseldorf, Germany; Interface Physics (E.E.v.F.), Faculty of Sciences, Utrecht University, The Netherlands; Department of Cardiology and Vascular Medicine (C.H., M.K.), University Hospital Düsseldorf, Germany; and Institute of Laser Medicine (D.H., M.M.), Heinrich-Heine-University of Düsseldorf, Germany.

Correspondence to Dr Christoph V. Suschek, Department of Plastic and Reconstructive Surgery, Hand Surgery, and Burn Center, Medical Faculty, RWTH Aachen University, Pauwelstraße 30, D-52074 Aachen, Germany. E-mail csuschek@ukaachen.de

Circulation Research **is available at http://circres.ahajournals.org** **DOI: 10.1161/CIRCRESAHA.109.207019**

Non-standard Abbreviations and Acronyms	
CALOS	cavity leak out spectroscopy
CLD	chemoluminescence detection
cPTIO	1*H*-imidazol-1-yloxy-2-(4-carboxyphenyl)-4,5-dihydro-4,4,5,5-tetramethyl-3-oxide
EPR	electron paramagnetic resonance
FBF	forearm blood flow
FMD	flow-mediated vasodilatation
HR	heart rate
MAP	mean arterial blood pressure
MNIC	mononitrosyl-iron complex
RS-NO	*S*-nitroso thiols
RX-NO	nitroso compounds

was independent of the endothelium.[7] Furthermore, photorelaxation was markedly potentiated by solutions containing nitrite,[8–10] indicating that under certain circumstances nitrite may exhibit relaxing activities comparable to NO.

Nitrite is a constituent of sweat, assumed to be formed on the skin surface by commensural bacteria.[11] Furthermore, in human skin NOS-dependent production of nitric oxide (NO) potentially occurs in all dermal cell types.[12,13] Some of the NO molecules formed remain at or close to the point of their origin as nitroso compounds, eg, *S*-nitrosothiols (RS-NO) or mercuric chloride–nonsensitive nitroso compounds or as the oxidation products nitrite and nitrate.[14] UVA is known to penetrate deep enough into skin to reach the micro vessels.[15,16] Thus, in human skin photosensitive NO derivates like RS-NOs or nitrite may undergo photodecomposition when irradiated with UVA light,[17–19] resulting in the formation of bioactive NO.[14,20] Previously, we have demonstrated that UVA exposure of healthy skin specimens leads to an enzyme-independent high-output NO formation, reaching concentrations comparable or higher than found with maximal activity of the inducible NO synthase in cytokine-activated human keratinocyte cultures in vitro.[21] We now extend these previous results by investigating the effect of whole body UVA exposure on the systemic blood circulation in humans.

Methods

Details regarding materials and experimental procedures with respect to materials, volunteers, UV sources, cell cultures, human skin samples, UVA-induced decomposition of nitrite and *S*-nitroso albumin formation, detection of *S*-nitroso proteins by immunohistochemistry, Western blot analysis of *S*-nitrosothiol proteins in human dermis, collection of blood samples and determination of blood pressure, cGMP measurements, analysis of cutaneous vascular parameters, sample preparation for detection of ^{15}N-labeled nitroso compounds in human blood plasma by cavity leak out spectroscopy (CALOS), detection of NO, quantification of nitrite and nitroso compounds by chemoluminescence detection (CLD), electron paramagnetic resonance (EPR) spectroscopy, detection of ^{15}NO by CALOS, and statistical analysis are in the expanded Methods section in the Online Data Supplement, available at http://circres.ahajournals.org.

Results

UVA Irradiation of Human Skin Reduces Blood Pressure

Immediately after UVA irradiation, as well as up to 60 minutes after the light stimulus, the values of systolic as well as diastolic blood pressure were reduced in all subjects as compared to control values determined before the irradiation procedure. Figure 1 shows that mean arterial blood pressure (MAP) was significantly lowered after UVA illumination. The effect persisted for a considerable duration: relaxation toward previous resting state was observed on the timescale of about an hour ($-5.6\pm3.2\%$ immediately after UVA, $-11.9\pm1.8\%$ 15 minutes after UVA, and $-5.9\pm2.1\%$ 45 minutes after UVA); $P<0.005$ as compared to the controls).

UVA Irradiation of Human Skin Increases Plasma Nitroso Compounds and Nitrite Concentrations

The blood plasma of UVA-irradiated volunteers showed significantly enhanced nitroso compound (RX-NO) (Figure 2), as well as nitrite concentrations (Figure 3), in the time interval of 15 to 45 minutes after illumination (RX-NO: $74\pm16\%$ 15 minutes after UVA and $53\pm19\%$ 45 minutes after UVA; $P<0.005$ as compared to the controls; nitrite: $43\pm22\%$ 15 minutes after UVA, $59\pm32\%$ 45 minutes after UVA, and $40\pm26\%$ 75 minutes after UVA; $P<0.005$ as compared to the controls). As shown in Figure 2D, UVA-induced decreases in blood pressure highly correlated with plasma RX-NO ($R^2=0.74$) but did not correlate with plasma nitrite ($R^2=0.0071$) concentration (Figure 3D).

UVA Irradiation of Human Skin Alters Cardiovascular Parameters

Furthermore, UVA-induced decrease in blood pressure was paralleled by increased forearm blood flow (FBF), increased flow-mediated vasodilatation of the brachial artery (FMDΔ%), as well as decreased forearm vascular resistance. As shown in Figure 4, 15 minutes after UVA, a significant increase in FBF ($26.1\pm7.3\%$) and FMDΔ% ($68\pm22\%$) and a significant decrease in forearm vascular resistance ($-28.1\pm7.5\%$) was detected. UVA challenge had no significant effects on heart rates of irradiated volunteers.

Plasma From UVA-Irradiated Volunteers Exerts NO-Dependent Biological Activity

cGMP responses of RFL-6 cells in the presence of superoxide dismutase (500 U/mL) and isobutyl methylxanthine (0.6 mmol/L) were used to determine the bioactivity of plasma obtained from nonirradiated as well as UVA-irradiated volunteers. As shown in Figure 4H, incubation of RFL-6 cells with plasma that was collected from UVA-exposed volunteers 30 minutes after the irradiation induced a significantly higher response in cGMP formation than plasma obtained from nonirradiated volunteers (7.07 ± 1.89 versus 2.65 ± 0.63 nmol/L cGMP per milligram of protein). These increases were significantly lower in the presence of the NO scavenger 1*H*-imidazol-1-yloxy-2-(4-carboxyphenyl)-4,5-dihydro-4,4,5,5-tetramethyl-3-oxide (cPTIO) (1.95 ± 1.23 nmol/L cGMP/mg protein).

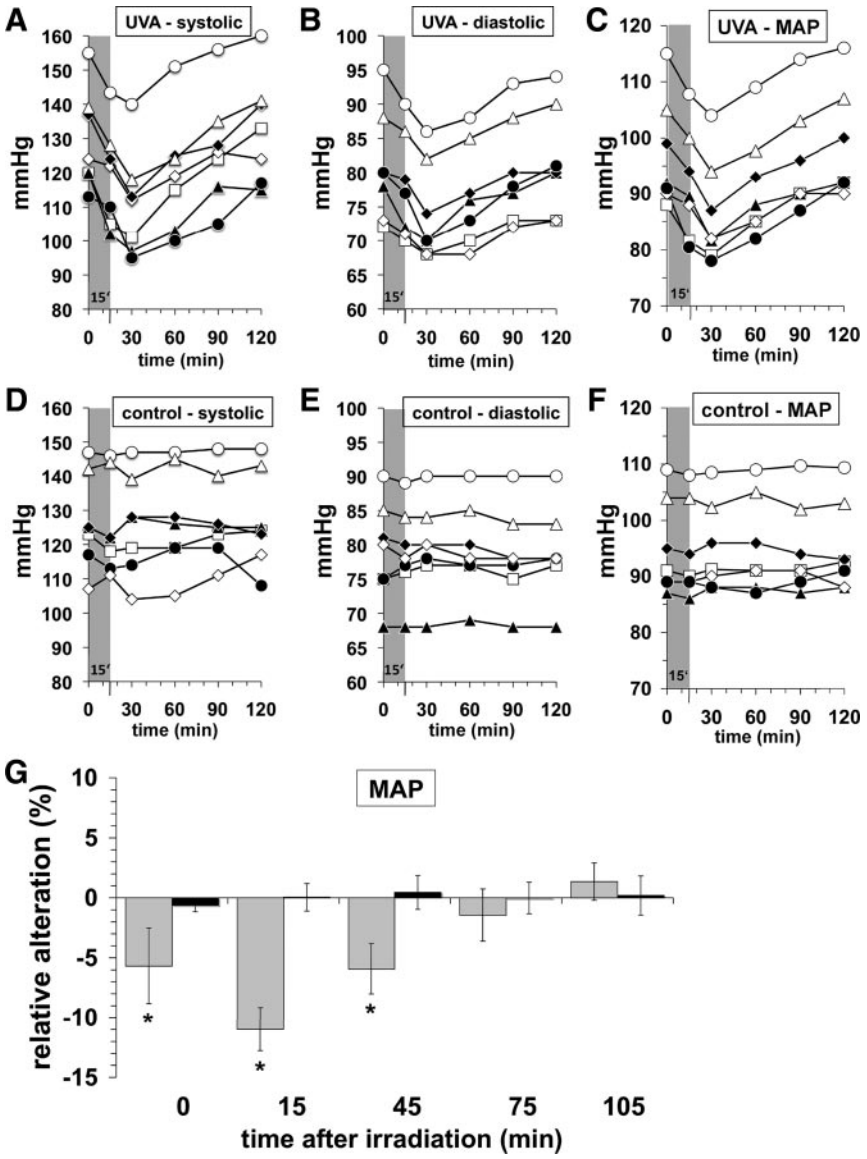

Figure 1. Effects of UVA irradiation of human skin on systolic and diastolic blood pressure. Healthy volunteers (○, no. 1; ●, no. 2; ◇, no. 3; ◆, no. 4; △, no. 5; ▲, no. 6; □, no. 7) were irradiated for 15 minutes (gray area in A through F) with UVA light (20 J/cm^2) or control-treated. Then, immediately after and 15, 45, 75, and 105 minutes after irradiation, systolic and diastolic blood pressure was detected. A, Systolic blood pressure in UVA-challenged volunteers. B, Diastolic blood pressure in UVA-challenged volunteers. C, MAP in UVA-irradiated volunteers. D, Systolic blood pressure in control-treated volunteers. E, Diastolic blood pressure in control-treated volunteers. F, MAP in control-treated volunteers. G, Relative alterations in MAP of irradiated (gray bars) and control volunteers (black bars) as compared to initial control values (0 minutes) indicated in C and F. Values are the means±SD of 7 individual experiments. *$P<0.001$.

Effects of Skin Temperature

During UVA irradiation, the ventral and lateral skin areas remained open to ambient air, and the skin temperatures of volunteers did not differ from controls (both 30.9±1.3°C). The dorsal skin areas were not ventilated by ambient air. Here, the skin temperature of irradiated volunteers (37.9±0.3°C) was slightly higher than that of controls (35.7±0.8°C) (Figure 5A). To exclude a possible artifact from skin temperature on blood pressure, we investigated the effect of a 15 minutes bath in 38°C instead of UVA irradiation. The warm bath did not affect blood pressure at any time points up to 105 minutes post bath. (Figure 5B).

Additionally, we measured capillary–venous oxygen saturation, blood filling, blood flow, and flow velocity in superficial (1 mm deep) and deeper (6 mm deep) microvessels of human skin before, immediately after and 30 minutes after exposure to UVA (20 J/cm^2) or 41°C warm water. As compared to nonirradiated skin, UVA exposure (20 J/cm^2) had no effects on the mentioned cutaneous vascular parameters (Figure 5C and 5D). As positive control, exposure of human skin for 10 minutes to 41°C warm water significantly enhanced blood flow and blood velocity of superficial (1 mm deep) and deeper (6 mm deep) microvessels of human skin (Figure 5E and 5F).

Concentrations of Nitrite and *S*-Nitrosothiols in Skin Specimens and in Plasma of Volunteers

In parallel, immunohistological analysis of human skin specimens revealed consistently the ubiquitous presence of *S*-nitrosated proteins (Figure 6A), whereas UVA irradiation of skin specimens leads to a consistent strong increase in *S*-nitrosothiols (Figure 6B). In normal human dermis, *S*-nitroso thiols can be found at a concentration of 3.2±0.9 μmol/L. The amount of *S*-nitroso thiols significantly increases after UVA challenge by 2.3-fold to 7.5±1.2 μmol/L (Figure 6D). A similar UVA-induced 2.9-fold enhancement was found for *S*-nitrosoalbumin in skin specimens (Figure 6E). In the dermis of humans skin specimens incubated for 12 hours with 100 μmol/L nitrite, UVA irradiation leads to a 4.5-fold increase in *S*-nitrosoalbumin levels as compared to control specimens (Figure 6E).

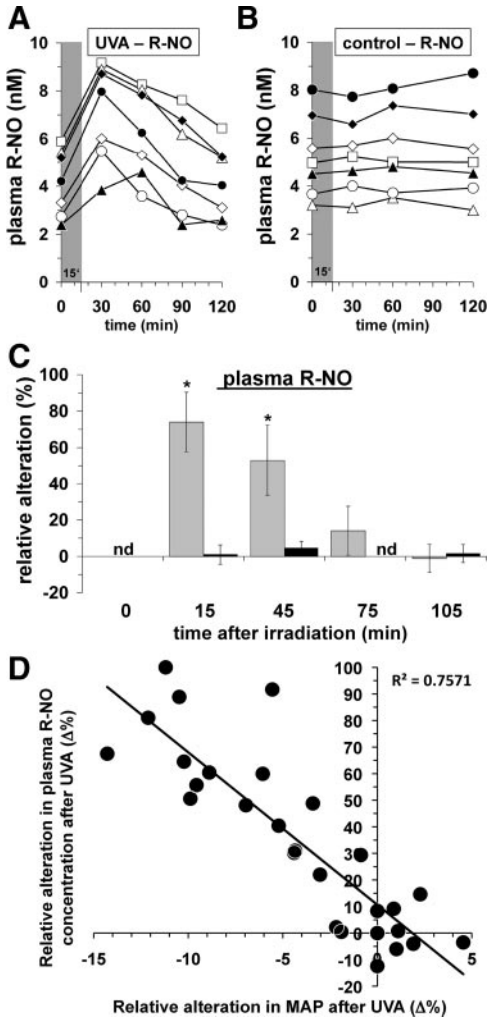

Figure 2. Effects of UVA irradiation of human skin on plasma concentrations of nitrosated compounds. Healthy volunteers (○, no. 1; ●, no. 2; ◇, no. 3; ◆, no. 4; △, no. 5; ▲, no. 6; □, no. 7) were irradiated for 15 minutes (gray area in A and B) with UVA light (20 J/cm^2) or control-treated. Then, 15, 45, 75, and 105 minutes after irradiation concentrations of nitrosated compounds (RX-NO) of plasma were detected by CLD. A, Plasma RX-NO concentrations of UVA-irradiated volunteers. B, Plasma RX-NO concentrations of control-treated volunteers. C, Relative alterations in plasma RX-NO concentrations of irradiated (gray bars) and control volunteers (black bars) as compared to initial control values (0 minutes) indicated in A and B. Values are the means±SD of 7 individual experiments. D, Correlation blot between MAP and plasma RX-NO concentration. With each volunteer, the calculated values of relative alterations of MAP after UVA irradiation as indicated in Figure 1G were correlated to the calculated values of relative alterations of plasma RX-NO as indicated in 2C. The correlation coefficient (R^2) is R^2=0.7419. *P<0.001.

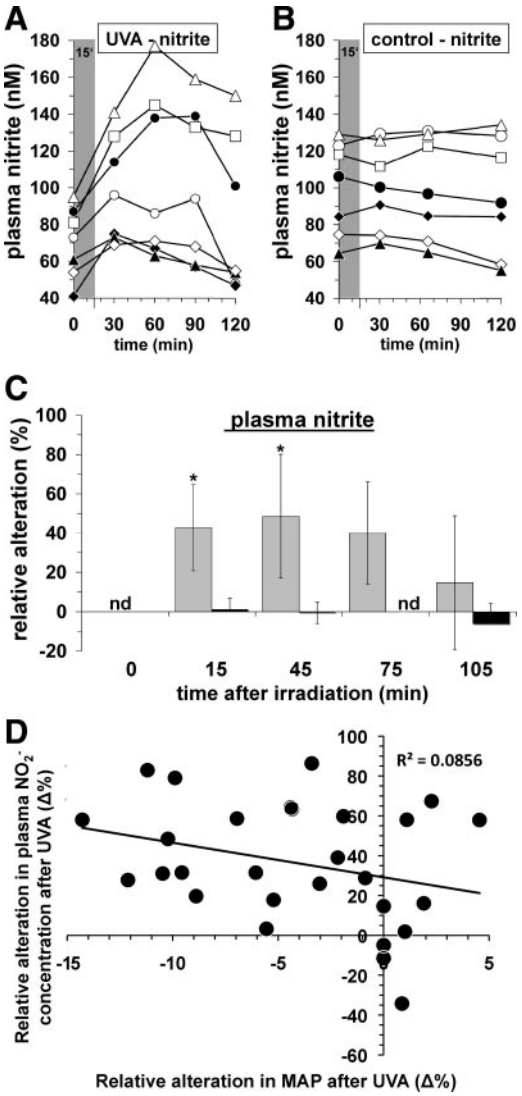

Figure 3. Effects of UVA irradiation of human skin on plasma nitrite concentrations. Healthy volunteers (○, no. 1; ●, no. 2; ◇, no. 3; ◆, no. 4; △, no. 5; ▲, no. 6; □, no. 7) were irradiated for 15 minutes (gray area in A and B) with UVA light (20 J/cm^2) or control-treated. Then, 15, 45, 75, and 105 minutes after irradiation nitrite concentrations of plasma were detected by CLD. A, Plasma nitrite concentrations of UVA-irradiated volunteers. B, Plasma nitrite concentrations of control-treated volunteers. C, Relative alterations in plasma nitrite concentrations of irradiated (gray bars) and control volunteers (black bars) as compared to initial control (c.) values indicated in A and B. Values are the means±SD of 7 individual experiments. D, Correlation blot between MAP and plasma nitrite concentration. With each volunteer, the calculated values of relative alterations of MAP after UVA irradiation, as indicated in Figure 1G, were correlated to the calculated values of relative alterations of plasma nitrite concentrations as indicated in 3C. The correlation coefficient (R^2) is R^2=0.0071. *P<0.001.

To demonstrate UVA-dependent nonenzymatic NO formation from nitrite as well as UVA-induced nitrite-dependent *S*-nitroso-thiol formation in vitro, we irradiated nitrite-containing (10 μmol/L) and/or BSA-containing (10 mg/mL) solutions (PBS, pH 7.4) with UVA and detected nonenzymatic NO formation by CLD and *S*-nitroso-BSA formation by Western blot. As shown in Figure 6F, at the physiological pH 7.4, UVA radiation led to an apparent nitrite decomposition and a significant formation of NO. Furthermore, in the presence of BSA this UVA-dependent nonenzymatic NO production from nitrite led to an significant increase in *S*-nitroso-BSA formation, as detected by the *S*-nitroso-cysteine-specific antiserum (Figure 6G).

Release of Gaseous NO From Intact Skin and NO Spin Trapping in Human Skin Specimens

In a further experiment, an airtight chamber (16 cm^2) with a UVA transparent front window was placed on the forearm of

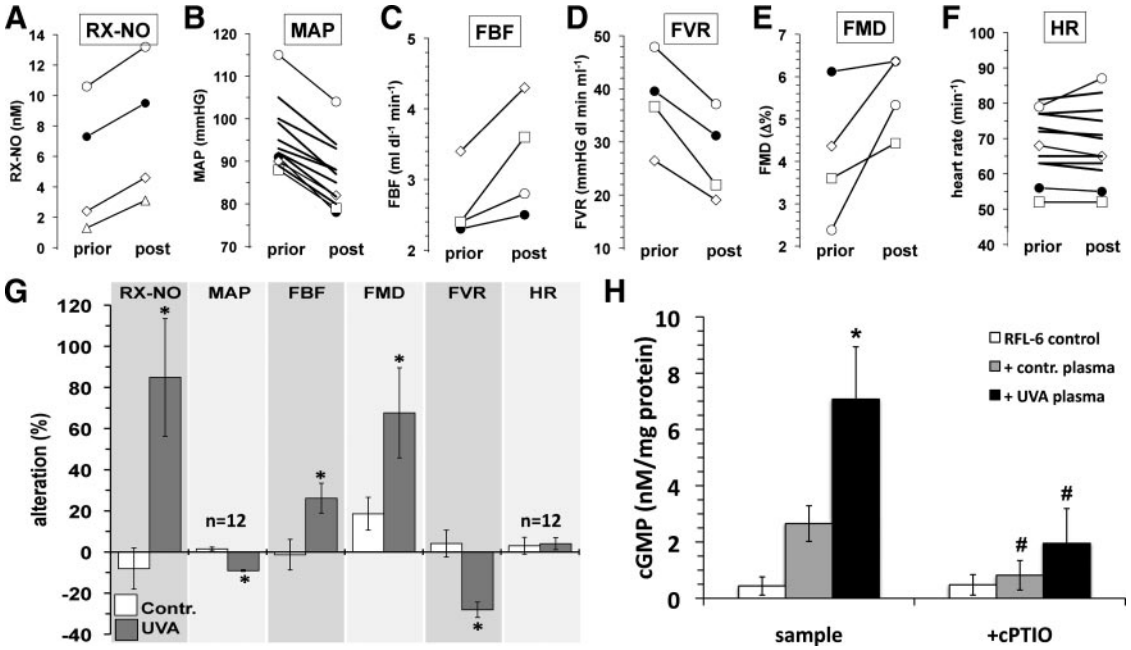

Figure 4. UVA irradiation of human skin alters cardiovascular parameters. Healthy volunteers (○, no. 1; ●, no. 2; ◇, no. 3; □, no. 7) were irradiated for 15 minutes with UVA light (20 J/cm^2). Prior and 15 minutes after (post) irradiation plasma RX-NO concentration (A), MAP (B), forearm blood flow (FBF) (C), forearm vascular resistance (FVR) (D), the diameter of the brachial artery (FMDΔ%) (E), and heart rate (F) was detected in parallel. Values are the means±SD of 4 or 12 individual (in B and F) experiments, respectively. G, Relative alterations in plasma RX-NO concentration, MAP, forearm blood flow (FBF), forearm vascular resistance (FVR), the diameter of the brachial artery (FMDΔ%), and heart rate of UVA-irradiated, as well as control-treated, volunteers as compared to initial control values (0 minutes). Values are the means±SD of 4 or 12 individual experiments, respectively. H, cGMP production of RFL-6 cells (3×10^5 cells) after 1 hour of incubation with plasma obtained from nonirradiated (gray bars), as well as UVA-irradiated (20 J/cm^2), volunteers (black bars, blood samples were collected 30 minutes after UVA challenge). White bars represent the constitutive cGMP production of RFL-6 cells alone. Additionally, incubations were performed in the presence of the NO scavenger cPTIO (40 μmol/L). Values represent the means±SD of 3 individual experiments. *$P<0.001$ as compared to the controls; #$P<0.001$ as compared to the respective samples incubated in the absence of cPTIO.

volunteers. A gas flow of helium collected the gaseous NO emanating from the skin and was fed into the CLD analyzer (Figure 7A). In absence of UVA, a basal release of 29±25 fmol of NO per second per square centimeter was detected. Under UVA illumination with 20 J/cm^2, the release of gaseous NO was enhanced fourfold to 148±55 fmol of NO per second per square centimeter ($P<0.001$). After application of skin cream containing 10 μmol/L nitrite, the photoinduced yield of gaseous NO was again significantly enhanced to 334±112 fmol of NO per second per square centimeter (Figure 7A).

After illumination of Fe^{2+}-DETC–loaded human skin specimens for 30 minutes with UVA light (25 J/cm^2), small sections of 200 to 250 mg were cut, immersed in strong HEPES buffer and snap frozen in liquid nitrogen. Before EPR analysis, the skin samples were reduced with dithionite (50 mmol/L for 15 minutes) to remove EPR signals from Cu^{2+}-DETC complexes.[22,23] The EPR spectra of figure 7B at test formation of mononitrosyl-iron complex (MNIC) adducts (^{14}NO-Fe^{2+}-DETC, hyperfine triplet at g=2.035) in human skin. Spectra of mamma skin specimens (Figure 8A through 8C) routinely showed additional signal from nitrosylated ferrous hemoglobin (paramagnetic NO-Fe^{2+}-Hb)[24] and ceruloplasmin.[25]

From comparison with calibrated reference samples, we estimated formation of 63±7 pmol MNIC in 200 mg male abdomen skin after 30 minutes UVA illumination. In absence of UVA, the MNIC yield remains below the EPR detection limit of ≈20 pmol. The MNIC yield could be enhanced to a massive 500 pmol by applying nitrite-loaded cream to the apical side of the skin specimens before UVA.

After splitting the skin samples horizontally with a razor blade, the apical outer layer had roughly threefold higher MNIC content than the endothermal inner layer. It shows that the outer layer is the main source of NO, as expected. Significantly, a large fraction of the total UVA induced NO has been trapped in the deeper skin layers, presumably because of diffusion of free NO through the skin tissue (The Fe-DETC traps and MNIC adducts themselves are immobilized in the lipid and protein compartments). After 30 minutes UVA, the MNIC concentration in the upper layers of male abdomen skin was ≈0.5±0.1 μmol/L. When the skin was pretreated with nitrite-spiked cream, the upper layers reached 6-fold higher MNIC concentration of ≈3.1±0.4 μmol/L.

These data suggest that NO is released from nitrite anions in the skin. Decomposition of nitrite was proven by application of cream with ^{15}N-nitrite (I=1/2) before UVA. The isotopic doublet structure of Figure 8 proved that the ^{15}NO ligand of MNIC derived from the ^{15}N-nitrite of the cream. After subtraction of an experimental ^{15}NO-Hb spectrum, we quantified the formation of 460 pmol ^{15}NO-Fe^{2-}-DETC in 240 mg of mamma skin (Figure 8b).

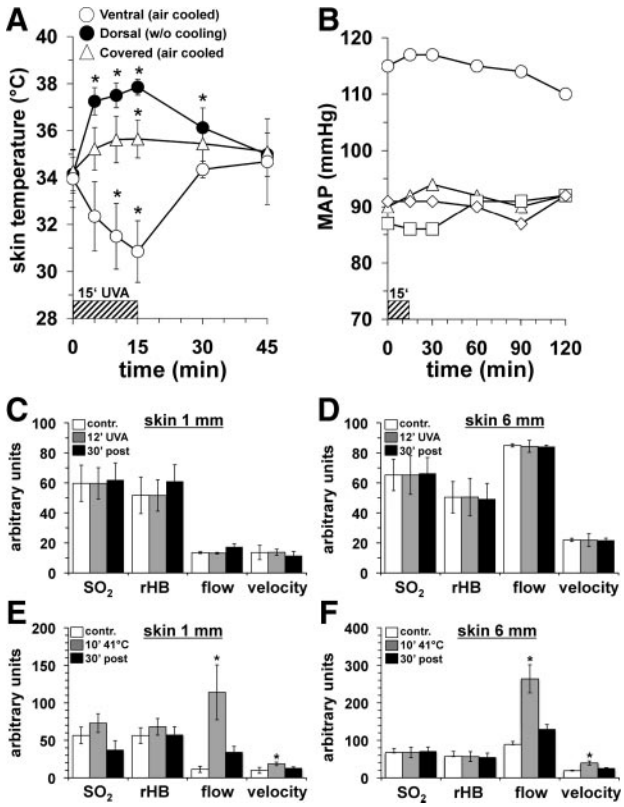

Figure 5. Effects of UVA irradiation on skin temperature, cutaneous blood flow, and influence of skin temperature on MAP. A, Skin temperature alterations were measured on UVA-exposed ventral and lateral air stream–ventilated skin areas and body sides (○), as well as UVA-irradiated dorsal skin areas that could not be cooled by the air stream (●). Additionally, skin temperature of control-treated subjects, which were covered during UVA exposure was measured (△). Values are the means±SD of 4 individual experiments. *$P<0.001$. The striped bar above the *x* axis indicates the time interval of light exposure. B, To exclude that the alterations in blood pressure after UVA challenge were the result of skin heating, blood pressure was determined during and after a 38°C bath for 15 minutes (○, ◇, □, △ represent the values of the respective volunteers). Striped bar indicates the time interval of warm water exposure. C and D, Effects of UVA radiation (20 J/cm^2) on capillary–venous oxygen saturation (SO_2), blood filling (rHB), blood flow (flow), and flow velocity (velocity) in superficial skin regions (1 mm) (C) and deeper skin tissue (6 mm) (D) before UVA challenge (white bars), immediately after the light stimulus (gray bars), and 30 minutes after UVA irradiation (black bars). E and F, Effects of warm water bath (41°C) on capillary–venous oxygen saturation (SO_2), blood filling (rHB), blood flow (flow), and flow velocity (velocity) in superficial skin regions (1 mm) (E) and deeper skin tissue (6 mm) (F) before warm water exposure (white bars), immediately after (gray bars), and 30 minutes after the warm water exposure (black bars). Values are the means±SD of 4 individual experiments. *$P<0.001$.

UVA Irradiation of Human Skin Induces Transmigration of Nitrite-Derived NO From Skin Tissue Into Plasma

Additional experiments were performed to identify the source of the NO moiety in the metabolites circulating in the blood of irradiated volunteers. Following application of skin cream with ^{15}N-nitrite (20 mL containing 100 μmol $Na^{15}NO_2$, 5 mmol/L), whole body UVA irradiation (20 J/cm^2) led to the formation of significant quantities of plasma ^{15}N-nitrite (40±4 nmol/L in controls versus 62±4 nmol/L in irradiated subjects, $P<0.001$) and *S*-nitrosothiols (RS-^{15}NO) (0.4±0.4 nmol/L in controls versus 1.7±0.9 nmol/L in irradiated subjects, $P<0.001$) (Figure 8E and 8D). These quantities were determined by the isotope-sensitive CALOS method. The fraction of labeled to unlabeled nitrite or nitroso compounds remained undetermined in this experiment.

Discussion

The key finding of the present study is that UVA irradiation of healthy human skin significantly increases intracutaneous NO and *S*-nitrosothiol concentrations via decomposition of cutaneous photolabile NO derivates with the result of significantly enhanced concentration of plasma nitroso compounds and a pronounced decrease in blood pressure.

Our observations of systemic UVA response can be plausibly explained by a mechanism comprising 3 elementary steps. First, UVA liberates NO from photolabile intracutaneous NO metabolites. Second, a fraction of the highly mobile NO diffuses toward the outer surface, where it escapes into the ambient atmosphere. (This fraction is detectable with the airtight skin chamber.) Another NO fraction diffuses to deeper tissue layers, where it enters the capillary vessels and enhances local levels of RS-NO. These nitrosated species may be low-molecular-weight, such as glutathione-*S*-NO, or protein-bound high-molecular-weight, such as albumin-S-NO. Third, the fairly stable nitroso compounds are distributed via the blood circulation, where it may elicit a systemic response like a drop in blood pressure. We note that the vasodilating and hypotensive properties of *S*-nitrosothiols are well documented.[26] The observed release of free NO from UVA-irradiated skin lends strong support to this mechanism. Using isotopically labeled ^{15}N-nitrite skin cream, CALOS spectroscopy demonstrated unequivocally that the photolysis of a photolabile NO derivate, here ^{15}N-nitrite, in the epidermis by UVA contributes to the formation of nitrite and RS-NO species in the systemic blood circulation of volunteers. It provides proof of principle that NO moieties generated in the upper skin layers may migrate to the interior and translocate to NO moieties in the blood circulation for our proposed mechanism in vivo.

Human skin tissue is known to contain significant quantities of nitrite (4 to 6 μmol/L), RS-NO (≈2.6 μmol/L) and mercuric chloride-resistant, as well as UVA-resistant, nitroso species (1.3 μmol/L).[14] These concentrations exceed the human plasma concentrations by several orders of magnitude (nitrite ≈20-fold, RS-NO ≈300 fold). Every cell types in human skin is able to produce NO by at least one of three NO synthases. Therefore, enzymatically generated NO represents an important source of cutaneous photolabile NO derivates. Nevertheless, recently data presented by Mowbray et al gave evidence that dietary nitrite and nitrate represent a more important source for cutaneous NO derivates.[27] Because dietary nitrate increases circulating nitrite concentrations,[28] it appears possible and feasible that dietary nitrate may also represent an effective way to boost skin reservoirs of photolabile NO species.

Using EPR spectroscopy, we, for the first time, give direct evidence here for UVA-induced intracutaneous NO formation via photodecomposition of endogenous sources of pho-

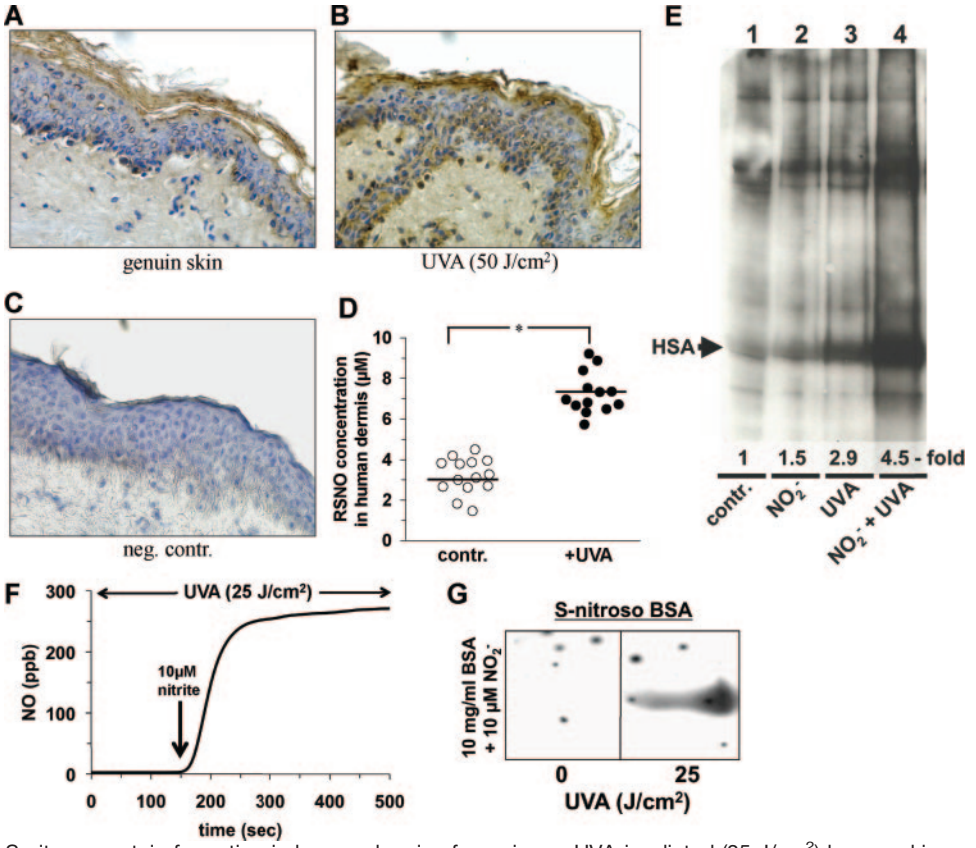

Figure 6. Analysis of *S*-nitrosothiols formation in human skin specimens, as well as in vitro and of UVA-induced photodecomposition of nitrite in aqueous solutions. In resting, as well as UVA-irradiated (25 J/cm^2), human skin specimens, obtained from mammoplastic surgery, *S*-nitrosation of proteins was detected by the *S*-nitrosocysteine-specific antiserum. A, Genuine human skin. B, UVA-irradiated skin specimens. C, For negative control, cryostat sections were denitrosated by a reducing solution (16 hours of incubation with 25 µmol/L $CuCl_2$ plus 1 mmol/L ascorbic acid in PBS, pH 7.4) before the antibody staining. A through C, Shown are representative pictures of 5 individual experiments. D, Detection of *S*-nitrosothiols in dermal tissue of genuine and UVA-irradiated human skin specimens detected by CLD in homogenates of genuine and UVA-irradiated human skin specimens. Values are the means±SD of 5 individual experiments. *$P<0.001$. E, Western blot analysis for *S*-nitroso protein formation in human dermis of genuine or UVA-irradiated (25 J/cm^2) human skin specimens maintained in the presence or absence of $NaNO_2$ (100 µmol/L). Shown is 1 representative graph of 3 individual experiments. F, In vitro nonenzymatic NO formation from UVA-irradiated (84 mW/cm^2) nitrite-containing solutions (10 µmol/L sodium nitrite in PBS, pH 7.4) detected by CLD. G, UVA-induced nitrite-dependent *S*-nitroso-thiol formation in vitro. UVA irradiation (25 J/cm^2) of PBS-containing (pH 7.4) nitrite (10 µmol/L sodium nitrite) and 10 mg/mL BSA resulted in an apparent *S*-nitroso-BSA formation, as detected by Western blot using a *S*-nitroso-cysteine–specific anti-serum.

tolabile NO derivates. The action of NO is largely determined by its rapid diffusion and its ability to penetrate cell membranes. The diffusion coefficient of NO at 37°C has been found to be 1.4-fold higher than that of oxygen or carbon monoxide and thus a diffusion distance of 500 µm was calculated for NO in tissue.[29] Thus, not surprisingly, with nitrite-enriched skin specimens, UVA-induced NO liberation could be found by EPR spectroscopy not only in apical skin regions but also in 2- to 3-mm deep regions of the dermis.

The penetration of photons into the skin strongly depends on the wavelength. It is known that UVA penetrates the epidermis and reaches even the deeper dermal regions down to 1 mm.[16] Approximately half of the UVA intensity can reach the depth of melanocytes and the dermal compartment,[30,31] and it has been estimated that the total solar energy deposited into the lower epidermis and upper dermis is 2 orders of magnitude higher for UVA than for UVB. In vitro studies have shown that UVA light at 340 to 360 nm induces the formation of NO by photolysis of nitrite anions, as well as *S*-nitrosated compounds, in aqueous solutions.[32–35] As shown by us previously,[14] UVA-induced photodecomposition of nitrite results in a modest but sustained release of NO. In contrast, irradiation of RS-NOs leads to a much elevated release of NO because of the far higher extinction coefficient of this species. Under high-UVA intensities, the release of NO is short-lived because of rapid depletion of RS-NO (photobleaching). It should be noted that neither nitrite nor $HgCl_2$-resistant nitroso compounds, probably *N*-nitrosated species (RNNOs), contribute to UVA-provoked NO release from human skin.[14] Detailed analysis of the mechanism of light-induced nitrite decomposition revealed the formation of very reactive and potentially cytotoxic radical species like $O_2^{-\cdot}$, $OH^{\bullet}$, or $NO_2^{\bullet}$.[17,32] The radical $NO_2^{\bullet}$ recombines rapidly ($k \approx 4.5\times10^8$ mol/L per second) with NO to N_2O_3. N_2O_3 and the catalytic action of transition metal ions represent very efficient nitrosating systems, in particular for thiols.[36,37] Via this reaction, $NO_2^{\bullet}$ decreases the yield of free NO from UVA-induced nitrite decomposition. In the presence of thiols such as glutathione, however, the NO-trapping capacity of $NO_2^{\bullet}$[38] will be counteracted via 3 reactions. First, N_2O_3 efficiently nitrosates thiols to RS-NO, which by itself is efficiently photolysed to NO and thiyl radicals ($^{-}S^{\bullet}$) under illumination by UVA. Secondly, $NO_2^{\bullet}$ will directly be reduced to nitrite by thiolates like GS^-. Thirdly, $^{-}S^{\bullet}$ reacts efficiently with GSNO to yield NO and a disulfide. In contrast, simple recombination of $GS^{\bullet}$ and $NO^{\bullet}$ has not been observed.[39] Therefore, reaction of thiols with both $NO_2^{\bullet}$ and with N_2O_3[38] will increase the formation of NO. The reaction of thiolate anions with $NO_2^{\bullet}$ is ≈10 times faster than the reaction with N_2O_3 (5×10^8 versus 6×10^7 mol/L per second) (reviewed elsewhere[38,40]).

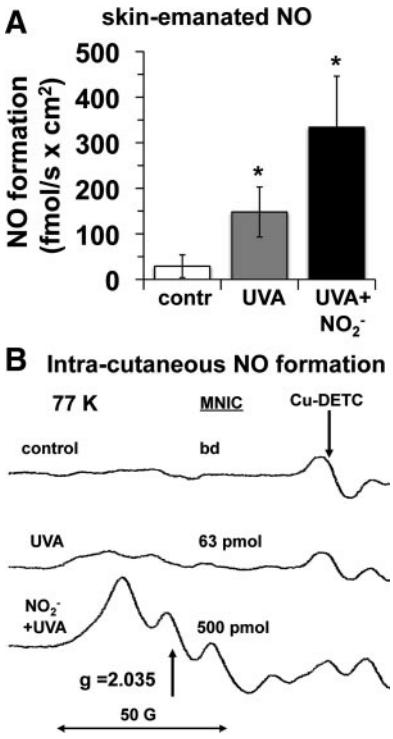

Figure 7. UVA irradiation of human skin increases emanation of cutaneous NO, as well as intracutaneous NO formation. A, Using an airtight chamber (16 cm^2) with a UVA transparent front window, which was placed on the forearm of volunteers, we collected the gaseous NO emanating from the skin and was fed into the CLD analyzer. In absence of UVA, a basal release of 29±25 fmol of NO per second per square centimeter was detected (white bar). Under UVA illumination with 20 J/cm^2, the release of gaseous NO was enhanced 4-fold to 148±55 fmol of NO per second per square centimeter (gray bar). After application of skin cream containing 10 μmol/L nitrite, the photoinduced yield of gaseous NO was again significantly enhanced to 334±112 fmol of NO per second per square centimeter (black bar). *$P<0.001$ as compared to the control (white bar). B, Fe^{2+}-DETC–loaded skin specimens from male abdomen were incubated for 30 minutes with 1 mmol/L *N*-iminoethyl-L-ornithine in the absence or presence of nitrite (100 μmol/L $NaNO_2$) and then were irradiated for 30 minutes with UVA light (25 J/cm^2). Intracutaneous formation of NO-Fe^{2+}-DETC complexes (MNIC) attributable to UVA-induced, nonenzymatic NO formation were detected by EPR spectroscopy. EPR spectra at 77 K of human skin specimens in HEPES buffer. The specimens are ≈200±10 mg each. In nonirradiated skin (control), MNIC signals are below the detection limit (bd) of ≈20 pmol. This spectrum shows the presence of ≈0.3 nmol of paramagnetic Cu^{2+}-DETC complexes. UVA irradiation of human skin tissue (UVA) induces the appearance of the EPR-typical triple signal for NO and a MNIC signal representing 63±6 pmol of MNIC. In the presence of nitrite, UVA irradiation of human skin (NO_2^-+UVA) leads to a MNIC signal, corresponding to 500±50 pmol of MNIC.

In parallel to UVA-induced intracutaneous NO formation, we observed a strong increase in cutaneous *S*-nitrosothiol formation in the epidermis, as well as in the deeper regions of the dermis. As shown by Western blot analysis, the dermal fraction of *S*-nitrosated compounds predominantly represent *S*-nitroso-albumin, which, because of absent circulation activity in the skin specimens, reflect the blood or serum filling, respectively, of cutaneous microvasculature. In vivo, of course, because of the excellent capillarization of the Stratum papillare, synthesized dermal *S*-nitroso-albumin will immediately leave the skin compartment. Functioning as a transport form for NO, *S*-nitroso-albumin will favor its rapid systemic distribution as well as its vasoavailability. *S*-nitroso-albumin has been previously proposed to act as a reservoir of NO within the circulation, transporting and releasing NO into vascular beds to cause vasodilation.[41,42]

Photoproduction of NO has been observed previously at these wavelengths in vascular tissue of rats,[33] and the action spectra of this photoproduction implicated endogenous *S*-nitrosothiols and nitrite as the source of NO. The UVA dose of 20 J/cm^2, as used here, was applied by using a commercial tanning facility. This dose remains significantly below the minimal erythemal UVA dose of 66±10 J/cm^2 reported for fair-skinned persons[43] and correlates with a sun exposure time of ≈45 minutes in a temperate climate zone.

UVA-induced effects on cardiovascular parameters, as well as the timescale of alterations, are in reasonable agreement with previous observations. Recently, Rassaf et al demonstrated that intravenous slow infusion of NO in healthy volunteers increased plasma levels of RS-NO and induced systemic hemodynamic effects at the level of both conduit and resistance vessels, as reflected by dilator responses in the brachial artery and forearm microvasculature, and elicits a simultaneous and significant drop in mean blood pressure. Interestingly, slow infusion of NO had no significant effects on heart rates of the treated volunteers.[44] These findings demonstrate that in humans, the pharmacological delivery of NO solutions results in the transport and delivery of NO as RS-NO along the vascular tree. Furthermore, in a pig model, Vilahur et al could show that low doses of *S*-nitroso glutathione (GS-NO), slowly administered, significantly reduced blood pressure.[45] In accordance with our observations, in both studies, heart rates were not significantly affected, neither by an NO nor low-dose RS-NO injection. In this context, it should be noted that the systemic response of the vascular system depends on whether the given dose is administrated by bolus injection or gradually with slow infusion. Thus, in the same study by Rassaf et al, an intravenous bolus injection of higher GS-NO amounts led to significantly enhanced heart rates.[44] Considering the time scale of UVA exposure, as well as of light-induced cardiovascular changes in our experimental setup, the underlying mechanism of our observations is less related to the high-dose GS-NO experiment of Rassaf et al but more to the mentioned NO and low dose RS-NO experiments.

As already mentioned, UVA radiation penetrates up to 1 mm into the skin. Therefore, hemodynamic changes shown here cannot be a direct result of cutaneous UVA exposure but rather are mediated by an UVA-induced factor. This assumption is strengthen by our observation that at the UVA doses used in our study, irradiation of skin did not show any significant local effects on cutaneous vasodilation or blood flow. Furthermore, we observed that an isolated irradiation of an arm, did not show any significant effects on blood pressure that was detected on this arm. On the other side, blood pressure detected on a nonirradiated arm of an otherwise UVA-irradiated volunteer shows the same results that were detected on the irradiated arm of the same volunteer (these

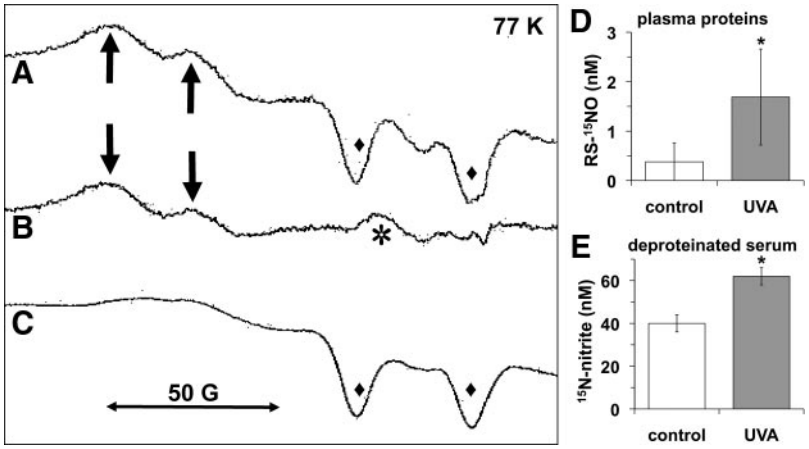

Figure 8. Effects of ^{15}N-nitrite cream on UVA-induced intracutaneous ^{15}NO formation and on RS-^{15}NO concentration in plasma of UVA-irradiated volunteers. Fe^{2+}-DETC–loaded human skin specimens, obtained from mammoplastic surgery, were treated apically for 30 minutes with 20 mL of a standard oil-in-water cream containing ^{15}N-nitrite (5 mmol/L $NaNO_2$) and then were irradiated for 30 minutes with UVA light (25 J/cm^2). Intracutaneous formation of ^{15}NO-Fe^{2+}-DETC complexes (MNIC) resulting from UVA-induced, nonenzymatic NO formation were detected by EPR spectroscopy. EPR spectrum of 240 mg of skin from female mamma was detected at 77 K. A, After reduction with dithionite, the sample shows a complex superposition of ^{15}N-MNIC (arrows) and ^{15}NO-Hb (♦). B, After numeric subtraction of an experimental spectrum of ^{15}NO-Hb (C), the difference spectrum (A minus C) shows ≈460 pmol of ^{15}N-MNIC (arrows) and some residual Cu^{2+}-DETC (*). C, The ^{15}NO-Hb spectrum used for the subtraction. D and E, Detection of ^{15}NO by CALOS. D, RS-^{15}NO concentrations in plasma of healthy volunteers, rubbed with a ^{15}N-nitrite–containing (5 mmol/L) cream before light exposure (20 J/cm^2 UVA). E, ^{15}N-nitrite concentrations in plasma of healthy volunteers, rubbed with a ^{15}N-nitrite–containing (5 mmol/L) cream before light exposure (20 J/cm^2 UVA). Values are the means±SD of 3 individual experiments. *$P<0.001$.

data are shown in the expanded Results section in the Online Data Supplement).

Furthermore, our control data strongly argue against an involvement of augmented ambient air temperature or skin temperature as an etiologic parameter for the effects on blood pressure observed after UVA challenge. In contrast to control-treated subjects, with UVA-irradiated volunteers, the permanent air stream exposure of ventral and lateral body parts, because of evaporation cooling, significantly decreases skin temperature. the surface of UVA-irradiated dorsal skin (not ventilated by cooling air), had a mean temperature of approx. 38±1°C. This is slightly higher than the skin temperature of fully covered subjects (35.7±0.8°C). Measuring capillary–venous oxygen saturation, blood filling, blood flow, and velocity of superficial (1 mm deep) and deeper (6 mm deep) microvessels of human skin clearly reveal that UVA exposure (20 J/cm^2) had no effects on the mentioned cutaneous vascular parameters, whereas, as positive control, exposure of human skin for 10 minutes to 41°C warm water significantly enhanced blood flow and blood velocity of superficial, as well as deeper, cutaneous microvessels. Moreover, mimicking skin temperature increases by a full-body bath in 38°C warm water for 15 minutes, none of the volunteers showed significant alterations in blood pressure. Thus, the influence of skin temperature-depended effect on blood pressure during UVA challenge can be neglected.

In conclusion, here, we give evidence that whole body UVA irradiation NO-dependently decreases blood pressure of healthy volunteers. These systemic effects are correlated with increased concentrations of nitroso compounds in the systemic circulation. We attribute the observed effects to photolysis of cutaneous nitrite and show that the physiological response may be enhanced by loading the skin with photolabile NO derivates before irradiation. Alternatively, endogenous photosensitive NO derivates may be modulated by control over dietary nitrate and nitrite intake.[46,47] These findings reveal the impact of light as an environmental parameter contributing to the phenomenon of "French paradox" and thus might have potential for the therapeutic applications in diseases with hypertension.

Sources of Funding

This work was supported by grants from the Federal Ministry of Education and Research ("BioLip" project), the Faculty of Medicine of the Heinrich-Heine-University Düsseldorf (Forschungskommission [FoKo program]), the Faculty of Medicine of the RWTH Aachen University (''START" program grant to C.O.), and the Interdisciplinary Centre for Clinical Research "BIOMAT" within the faculty of Medicine at the RWTH Aachen University (grant K3 to C.V.S.).

Disclosures

None.

References

1. Burke AP, Farb A, Liang YH, Smialek J, Virmani R. Effect of hypertension and cardiac hypertrophy on coronary artery morphology in sudden cardiac death. *Circulation*. 1996;94:3138–3145.
2. Levy D, Larson MG, Vasan RS, Kannel WB, Ho KKL. The progression from hypertension to congestive heart failure. *JAMA*. 1996;275:1557–1562.
3. Intersalt: an international study of electrolyte excretion and blood pressure. Results for 24 hour urinary sodium and potassium excretion. Intersalt Cooperative Research Group. *BMJ*. 1988;297:319–328.
4. Rostand SG. Ultraviolet light may contribute to geographic and racial blood pressure differences. *Hypertension*. 1997;30:150–156.
5. Furchgott RF, Ehrreich SJ, Greenblatt E. The photoactivated relaxation of smooth muscle of rabbit aorta. *J Gen Physiol*. 1961;44:499–519.
6. Ehrreich SJ, Furchgott RF. Relaxation of mammalian smooth muscles by visible and ultraviolet radiation. *Nature*. 1968;218:682–684.
7. Furchgott RF, Martin W, Jothianandan D, Villani GM. Comparison of endothelium-dependent relaxation by acetylcholine and endothelium-independent relaxation by light in the rabbit aorta. In: Paton W, Mitchell J, Turner P, eds. *Proceedings of the IUPHAR 9th International Congress of Pharmacology*. London, United Kingdom: Macmillan Press; 1984:148–158.
8. Furchgott RF. Endothelium-dependent relaxation, endothelium-derived relaxing factor and photorelaxation of blood vessels. *Semin Perinatol*. 1991;15:11–15.
9. Furchgott RF, Jothianandan D. Endothelium-dependent and -independent vasodilation involving cyclic GMP: relaxation induced by nitric oxide, carbon monoxide and light. *Blood Vessels*. 1991;28:52–61.
10. Wigilius IM, Axelsson KL, Andersson RG, Karlsson JO, Odman S. Effects of sodium nitrite on ultraviolet light-induced relaxation and ultra-

violet light-dependent activation of guanylate cyclase in bovine mesenteric arteries. *Biochem Biophys Res Commun*. 1990;169:129–135.
11. Weller R, Pattullo S, Smith L, Golden M, Ormerod A, Benjamin N. Nitric oxide is generated on the skin surface by reduction of sweat nitrate. *J Invest Dermatol*. 1996;107:327–331.
12. Bruch-Gerharz D, Ruzicka T, Kolb-Bachofen V. Nitric oxide in human skin: current status and future prospects. *J Invest Dermatol*. 1998; 110:1–7.
13. Bruch-Gerharz D, Ruzicka T, Kolb-Bachofen V. Nitric oxide and its implications in skin homeostasis and disease - a review. *Arch Dermatol Res*. 1998;290:643–651.
14. Paunel AN, Dejam A, Thelen S, Kirsch M, Horstjann M, Gharini P, Murtz M, Kelm M, de Groot H, Kolb-Bachofen V, Suschek CV. Enzyme-independent nitric oxide formation during UVA challenge of human skin: characterization, molecular sources, and mechanisms. *Free Radic Biol Med*. 2005;38:606–615.
15. Holick MF. Photosynthesis of vitamin D in the skin: effect of environmental and life-style variables. *Fed Proc*. 1987;46:1876–1882.
16. Tyrrell RM. UVA (320–380 nm) as an oxidative stress. In: Sies H, ed. *Oxidative Stress, Oxidants and Antioxidants*. London, United Kingdom: Academic Press; 1991:57–83.
17. Zafiriou OC, Bonneau R. Wavelength-dependent quantum yield of OH radical formation from photolysis of nitrite ion in water. *Photochem Photobiol*. 1987;45:723–727.
18. Strehlow H, Wagner I. Flash photolysis in aqueous nitrite solutions. *Z Phys Chem*. 1982;132:151–160.
19. Treinin A, Hayon E. Absorption spectra and reaction kinetics of NO2, N2O3, and N2O4 in aqueous solution. *J Am Chem Soc*. 1970;92: 5821–5828.
20. Suschek CV, Schroeder P, Aust O, Sies H, Mahotka C, Horstjann M, Ganser H, Murtz M, Hering P, Schnorr O, Kroncke KD, Kolb-Bachofen V. The presence of nitrite during UVA irradiation protects from apoptosis. *FASEB J*. 2003;17:2342–2344.
21. Bruch-Gerharz D, Schnorr O, Suschek C, Beck KF, Pfeilschifter J, Ruzicka T, Kolb-Bachofen V. Arginase 1 overexpression in psoriasis: limitation of inducible nitric oxide synthase activity as a molecular mechanism for keratinocyte hyperproliferation. *Am J Pathol*. 2003;162: 203–211.
22. Vanin AF, Bevers LM, Mikoyan VD, Poltorakov AP, Kubrina LN, van Faassen E. Reduction enhances yields of nitric oxide trapping by iron-diethyldithiocarbamate complex in biological systems. *Nitric Oxide*. 2007;16:71–81.
23. van Faassen EE, Koeners MP, Joles JA, Vanin AF. Detection of basal NO production in rat tissues using iron-dithiocarbamate complexes. *Nitric Oxide*. 2008;18:279–286.
24. Kosaka H, Shiga T. Detection of nitric oxide by electron spin resonance using haemoglobin. In: Feelisch M, Stamler JS, eds. *Methods of Nitric Oxide Research*. New York: John Wiley & Sons Inc; 1996.
25. Jaszewski AR, Fann YC, Chen YR, Sato K, Corbett J, Mason RP. EPR spectroscopy studies on the structural transition of nitrosyl hemoglobin in the arterial-venous cycle of DEANO-treated rats as it relates to the proposed nitrosyl hemoglobin/nitrosothiol hemoglobin exchange. *Free Radic Biol Med*. 2003;35:444–451.
26. Rassaf T, Kelm M. Nitrite and nitrosospecies in blood and tissue: approaching the gap between bench and bedside. In: van Faassen EE, Vanin AF, eds. *Radicals for Life: The Various Forms of Nitric Oxide*. Amsterdam, The Netherlands: Elsevier; 2007:269–288.
27. Mowbray M, McLintock S, Weerakoon R, Lomatschinsky N, Jones S, Rossi AG, Weller RB. Enzyme-independent NO stores in human skin: quantification and influence of UV radiation. *J Invest Dermatol.* 2009; 129:834–842.
28. Lundberg JO, Govoni M. Inorganic nitrate is a possible source for systemic generation of nitric oxide. *Free Radic Biol Med*. 2004;37: 395–400.
29. Dawson TM, Snyder SH. Gases as biological messengers: nitric oxide and carbon monoxide in the brain. *J Neurosci*. 1994;14:5147–5159.
30. Bruls WAG, Vanweelden H, Vanderleun JC. Transmission of UV-radiation through human epidermal layers as a factor influencing the minimal erythema dose. *Photochem Photobiol*. 1984;39:63–67.
31. Kaidbey KH, Agin PP, Sayre RM, Kligman AM. Photo-protection by melanin - comparison of black and caucasian skin. *J Am Acad Dermatol*. 1979;1:249–260.
32. Fischer M, Warneck P. Photodecomposition of nitrite and undissociated nitrous acid in aqueous solution. *J Phys Chem*. 1996;100:18749–18756.
33. Rodriguez J, Maloney RE, Rassaf T, Bryan NS, Feelisch M. Chemical nature of nitric oxide storage forms in rat vascular tissue. *Proc Natl Acad Sci U S A*. 2003;100:336–341.
34. Sexton DJ, Muruganandam A, McKenney DJ, Mutus B. Visible light photochemical release of nitric oxide from S-nitrosoglutathione: potential photochemotherapeutic applications. *Photochem Photobiol*. 1994;59: 463–467.
35. Zhelyaskov VR, Gee KR, Godwin DW. Control of NO concentration in solutions of nitrosothiol compounds by light. *Photochem Photobiol*. 1998;67:282–288.
36. van Faassen EE, Vanin AF. Low-molecular-weight S-nitrosothiols. In: van Faassen EE, Vanin AF, eds. *Radicals for Life: The Various Forms of Nitric Oxide*. Amsterdam, The Netherlands: Elsevier; 2007:173–199.
37. Yang Y, Loscalzo J. S-nitrosated proteins: formation, metabolism, and function. In: van Faassen EE, Vanin AF, eds. *Radicals for Life: The Various Forms of Nitric Oxide*. Amsterdam, The Netherlands: Elsevier; 2007:201–221.
38. Kirsch M, Korth HG, Sustmann R, de Groot H. The pathobiochemistry of nitrogen dioxide. *Biol Chem*. 2002;383:389–399.
39. Wood PD, Mutus B, Redmond RW. The mechanism of photochemical release of nitric oxide from S-nitrosoglutathione. *Photochem Photobiol.* 1996;64 518–524.
40. Kirsch M, de Groot H. Formation of peroxynitrite from reaction of nitroxyl anion with molecular oxygen. *J Biol Chem*. 2002;277: 13379–13388.
41. Keaney JF, Simon DI, Stamler JS, Jaraki O, Scharfstein J, Vita JA, Loscalzo J. No forms an adduct with serum-albumin that has endothelium-derived relaxing factor like properties. *J Clin Invest*. 1993;91: 1582–1589.
42. Scharfstein JS, Keaney JF, Slivka A, Welch GN, Vita JA, Stamler JS, Loscalzo J. In-vivo transfer of nitric-oxide between a plasma protein-bound reservoir and low-molecular-weight thiols. *J Clin Invest*. 1994;94:1432–1439.
43. Paul BS, Parrish JA. The interaction of UVA and UVB in the production of threshold erythema. *J Invest Dermatol*. 1982;78:371–374.
44. Rassaf T, Kleinbongard P, Preik M, Dejam A, Gharini P, Lauer T, Erckenbrecht J, Duschin A, Schulz R, Heusch G, Feelisch M, Kelm M. Plasma nitrosothiols contribute to the systemic vasodilator effects of intravenously applied NO - experimental and clinical study on the fate of NO in human blood. *Circ Res*. 2002;91:470–477.
45. Vilahur G, Baldellou MI, Segales E, Salas E, Badimon L. Inhibition of thrombosis by a novel platelet selective S-nitrosothiol compound without hemodynamic side effects. *Cardiovasc Res*. 2004;61:806–816.
46. Lundberg JO, Weitzberg E, Gladwin MT. The nitrate-nitrite-nitric oxide pathway in physiology and therapeutics. *Nat Rev Drug Discov*. 2008;7: 156–167.
47. Larsen FJ, Ekblom B, Sahlin K, Lundberg JO, Weitzberg E. Effects of dietary nitrate on blood pressure in healthy volunteers. *N Engl J Med*. 2006;355:2792–2793.

Supplement Material

EXTENDED MATERIALS AND METHODS

Materials

If not other indicated all chemicals were from Sigma (Deisenhofen, Germany), the peroxidase-conjugated goat anti rabbit IgG antibody and the isotype-matched non-relevant rabbit anti-serum were from Calbiochem (Luzern, Switzerland). Gaseous NO was determined using the chemiluminescence detector (CLD 77 Amsp) from Eco Physics (Ann Arbor, MI, USA)

Volunteers

The protocol was approved by the ethics committee of the Medical Faculty of the Heinrich-Heine University of Düsseldorf and conducted in compliance with the Declaration of Helsinki Principles.

Fair skinned volunteers with skin type 2-3 [1], 2 female, 8 male, age 38±11 years, body-mass index 26±4 kg/cm^2 were recruited from the student population and staff members.

UV sources

Irradiation of human skin specimens *in vitro* was performed using a 4000 W mercury arc lamp unit from Sellas Medizinische Geräte (Gevelsberg, Germany) emitting a UVA_1-spectrum (340 – 410 nm) with a maximum of intensity at 366 nm (the lamp was used in a distance of 35 cm from the sample corresponding to a radiant flux intensity of 84 mW/cm^2). The UVA dose in the *in vitro* experiments was 25 J/cm^2.

The IK ERGOLINE 44 sun-tube (Ergoline GmbH, Windhagen, Germany) was used for whole-body irradiation. This air-conditioned tanning device was fitted with 44 Solarium Plus R 100 W fluorescence lamps (Wolff System AG, Riegel, Germany) emitting UVA-light (99.3% of UV at wavelengths >320 nm and 84% >340 nm) with a

maximum intensity at 355 nm. The integrated irradiance at skin level was 19.5± 0.9 mW/cm^2 for UVA and 0.05 ± 0.01mW/cm^2 UVB (means from 40 measure sites). The UVA dosage for whole body irradiation was 20 J/cm^2. This dosage was given in line with the manufacturer's recommendations and corresponds to the UVA contents of approx. 45 minutes sun exposure in a temperate climate zone. During UVA-exposure volunteers lying in horizontal position were irradiated from all sides. While the cooling air stream was able to cool head, neck, arms, legs as well as the ventral and lateral parts of the body, the dorsal body areas of pad contact were not ventilated.
Volunteers only wore goggles that were opaque to UV and visible light.
Control-treatment was performed by UVA-irradiation of dressed volunteers encased with UV-light-impermeable cloths. During irradiation a constant ambient temperature-interval within the sunbed-tube of 29±1 °C was achieved by manual adjustment of the integrated air-condition.
Skin surface temperature was measured within 0.5 °C with a contact thermometer (Testo, T-stripe, Vienna, AU).
Every volunteer contributed to dressed and undressed experiments (crossover experiment).

Cell cultures

Rat lung fibroblastoma cells (RFL-6) were grown in Dulbecco's modified Eagle's medium (DMEM) supplemented with 10% bovine calf serum, 100 U/ml penicillin, and 100 µg/ml streptomycin. Cells were grown on 10 cm culture dishes and were used for experiments after reaching confluency.

Human skin samples

Human skin specimens were derived from mammoplastic or abdominoplastic surgery, cut into 10-mm squares, embedded immediately in Tissue-Tek (Reichert-Jung, Vienna, Austria), and snap frozen in liquid nitrogen for immunohistochemical

characterization. In order to examine S-nitrosoprotein concentrations in human dermis, skin specimens were incubated overnight (15 h) with Dispase (15 mg/ml; Boehringer, Mannheim, Germany) at 4°C and then epidermis was detached from the dermis.

The concentrations of cutaneous NO-derived products or reduced thiols were analyzed in the supernatants of skin homogenates. For this purpose embedded skin specimens (10-mm squares) were cryo-cut parallel to the epidermis into 20 µm thin slices down to a depth of 2 mm into the dermis (100 sections). The material was then weighed, diluted in 3 w/vol. of NEM-buffer (PBS containing 5 mM N-ethyl-maleimide (NEM), 2.5 mM EDTA, protease inhibitor), and homogenized. After a short centrifugation step the supernatants were collected, diluted to a protein content of 10 mg/ml, and immediately used or frozen at -20°C for maximally two weeks.

In addition, aliquots of fresh skin specimens (5-mm squares) were taken in short-time organ culture and were maintained in the RPMI1640/20% FCS culture medium (pH 7.4) in the dark up to 96 hours without loss of cell viability or function exactly as described by us previously.[2]

UVA-induced decomposition of nitrite and S-nitroso albumin formation

In order to demonstrate non-enzymatic NO-formation from aqueous nitrite solutions as a result of UVA-irradiation we irradiated PBS (pH 7.4) containing sodium nitrite (10 µM) with UVA (84 mW/cm^2 in a distance of 35 cm from the sample). UVA-irradiation of the solutions (in total 20 ml) was performed in a quartz glass cylinder (120-cm^3 glass cylinder with 3.3-cm diameter), permanently exhausting of the gases for detection of NO by CLD exactly as described previously.[3]

Additionally, in order to demonstrate nitrite-dependent S-nitroso-thiol formation as a result of UVA-irradiation we irradiated PBS (pH 7.4) containing sodium nitrite (10 µM) and 10 mg/ml bovine serum albumin (BSA) with UVA (25 J/cm^2). S-nitrosation of BSA was detected by Western-Blot and using a *S*-nitrosocysteine-specific rabbit anti-

serum exactly as described below.

Detection of *S*-nitroso proteins by immunohistochemistry

In resting as well as UVA-irradiated (25 J/cm^2) human skin specimens S-nitrosation of proteins was examined using a *S*-nitrosocysteine-specific rabbit anti-serum. Skin specimens were embedded, snap frozen, and cryostat sections (7 µm of thickness) were prepared using a micro-cryotom exactly as described earlier.[4] Cryostat sections were fix by glutaraldehyde (0.2% in TBS, pH 7.0) for 15 min at 4° in a moist chamber, followed by inhibition of endogenous peroxidase activity with 0.3% H_2O_2 in ethanol, and washed three times in TBS. In order to stabilize S-nitrosothiols, transnitrosation was inhibited by alkylation of reduced thiols. Therefore, fixed sections were incubated for two hours in the dark with 10 mM NEM plus 0.3 % Triton X-100 in PBS. After blocking of unspecific binding with 0.5% BSA in TBS for 30 min and rinsing, specimens were incubated with the previously described rabbit anti-*S*-nitrosocysteine anti-serum [5, 6] used in a 1:100 dilution in TBS (supplemented with 3% low-fat milk powder and 0.5% Tween 20, pH 7.4). As secondary antibody peroxidase-conjugated goat anti rabbit IgG was used in a final dilution of 1:30 for one hour in TBS. All steps were performed at 4°C. For negative control S-nitrosothiols on cryostat sections were denitrosated by incubating the sections overnight (16 h) in the dark at 25°C in PBS containing 1 % $CuSO_4$ or 0.2 % $HgCl_2$ plus 0.5 % Sulfanilamid (diluted in 1N HCl) plus 2 % SDS. Then sections were washed using the washing buffer (0.1 mM diethylene triamine pentaacetic acid, DTPA plus 0.3 % Triton X-100 in PBS). After an additional washing in TBS nuclei were stained with hematoxylin for 1 min. Then, samples were incubated with 0.05% diaminobenzidine + 0.015% H_2O_2 for 5 minutes at room temperature. For light microscopy, cell samples were dehydrated, cleared with xylene and embedded in Eukitt.

Western-Blot-analysis of S-nitrosothiol proteins in human dermis

In order to examine S-nitrosoprotein formation in human dermis, skin specimens were irradiated by UVA (25 J/cm^2) in the presence or absence of $NaNO_2$ (100 µM), incubated overnight (15 h) with Dispase (15 mg/ml; Boehringer, Mannheim, Germany) at 4°C. After detaching the epidermis homogenate solutions (10 mg protein/ml) of the dermis were prepared. In each lane of a 10%-Bis-Tris NuPAGE Novex pre-cast polyacrylamide gel (Invitrogen, Karlsruhe, Germany) 35 µl (35 µg protein) of skin homogenates were separated by electrophoresis using the NuPAGE electrophoresis system (Invitrogen, Karlsruhe, Germany) and the MOPS-SDS running buffer system under non-reducing conditions. Then protein was blotted on a nitrocellulose membrane using the NuPAGE transfer buffer (25 mM Bis-Tris, 25 mM Bicine, 1 mM EDTA, 20% methanol, pH 7.2) and following the manufactures instructions. Protein was visualized by using S-nitroso-specific anti-sera.[5, 6] Further incubations of the blots were: 2 hours with blocking buffer (2% BSA, 5% non fat milk powder, 0.1% Tween 20 in PBS-buffer), 30 min at room temperature with a 1:100 dilution of the anti-S-nitroso anti-serum, and 30 minutes with a 1:2000 dilution of the secondary horseradish peroxidase conjugated antibody. Finally, blots were incubated for 5 minutes in ECL reagent (Pierce, Rockford, IL, USA), and exposed to an autoradiographic film.

Collection of blood samples and determination of blood pressure

During the whole experimental procedure - from 45 minutes prior until 120 minutes post UVA-challenge - volunteers were kept in supine position. Then, 30 minutes prior to UVA-irradiation as well as 15, 45, 75 and 105 minutes after the light exposure venous blood samples (2 x 10 ml) were collected from the right cubatal vein. Systolic and diastolic blood pressure was determined by a cardiologist at the time points -30, -15, 0 minutes prior the irradiation, immediately after irradiation as well as 15, 45, 75, and 105 minutes after UVA-exposure by the method of Riva-Rocci using

a mercury sphygmomanometer or the OMRON M6 Automatic Digital Blood Pressure Monitor (OMRON Medizintechnik, Mannheim, Germany). Blood pressure, calculated as average of three successive measurements, always was determined at the right upper arm. Mean arterial pressure (MAP) was calculated as MAP $\simeq$ DP + 1/3 (SP-DP) where SP is systolic pressure and DP is diastolic pressure.

Changes in forearm blood flow (FBF) were measured at 10-second intervals using standard techniques of mercury-in-rubber strain-gauge plethysmography.[7] The diameter of the brachial artery (FMDΔ%) was measured with a 15-MHz linear array transducer proximal above the antecubital fossa at end diastole by an automated analysis system.[8] We calculated forearm vascular resistance (FVR) by dividing the mean arterial pressure by FBF.

cGMP-measurement

Guanosine 3',5'-cyclic monophosphate (cGMP) responses of RFL-6 cells in the presence of superoxide dismutase (500 U/ml) and isobutylmethylxanthine (0.6 mM) were used to determine the bioactivity of plasma obtained from non-irradiated as well as UVA-irradiated volunteers NO.[9] RFL-6 monolayers ($3x10^5$ cells) were covered with 1 ml plasma prepared from blood samples of healthy volunteers or from blood samples from UVA-irradiated volunteers collected 30 minutes after UVA (20 J/cm^2) exposure in the presence or absence of the NO scavenger 1*H*-imidazol-1-yloxy-2-(4-carboxyphenyl)-4,5-dihydro-4,4,5,5-tetramethyl-3-oxide (cPTIO, 40 µM; Alexis Biochemicals, Grünberg, Germany). After 60 min of incubation cells were scratched and lysed by repeated freezing and thawing. cGMP levels in the supernatants were detected using the cGMP-specific ELISA (R&D-Systems, Wiesbaden, Germany) following the manufactures recommendation and were calculated as nM cGMP/mg protein.

Analysis of cutaneous vascular parameters

Effects of UVA radiation and warm water bath of cutaneous vascular parameters were performed using the O2C-device (LEA Medizintechnik GmbH, Giessen, Germany). O2C is a diagnostic device for non-invasive determination of perfusion of tissue, capillary-venous oxygen saturation, blood flow velocity, and blood filling of microvessels in microcirculation of blood perfused tissues. O2C is a multiple channel system which makes it possible to determine perfusion quantities and oxygen values by two chanels. Channel 1 records the mentioned parameters in the superficial skin regions, while channel 2 monitors the different values of deeper skin tissue.

Sample preparation for detection of ^{15}N-labeled nitroso compounds in human blood plasma by CALOS

In order to analyze the mechanism of the translocation of non-enzymatically produced NO from the skin into the circulation, 20 ml of a basis cream (standard oil-in-water-cream) containing ^{15}N-labeled nitrite (5 mM $Na^{15}NO_2$, 98%$_{atom}$ ^{15}N) was evenly spread on the entire skin of healthy volunteers. The cream totally entered into skin leaving an essentially dry surface within 15 minutes. After a residence time of 45 minutes test persons were UVA-irradiated or control-treated exactly as mentioned above. Venous blood samples (20 ml) were collected 10 minutes prior to the irradiation procedure (control) and 15 minutes after finishing the irradiation. Immediately, after collection, blood samples were centrifuged (10 min at 800 x g, 4°C), the cellular fraction was discarded, and plasma was mixed with two volumes of cold (-20°C) acetone. Precipitated proteins were separated by centrifugation (10 min at 3200 x g, 4°C), protein pellets were washed twice with cold (-20°C) acetone, and resolved in PBS. In the deproteinized plasma fraction acetone was removed by overnight vacuum evaporation. Then protein-containing solutions as well as the deproteinized plasma were incubated for 60 min with nitrate reductase (0.15 U/ml in PBS containing 2.7 µM NADPH, 1.35 mM glucose-6-phosphate, 0.4 U/ml glucose-6-

phosphate dehydrogenase).[10] In order to detect the grade of protein S-nitrosation in the protein fraction or nitrite in the deproteinized plasma, respectively, we used the iodine/iodide reduction system as described above, whereas the liberated ^{15}NO was detected by cavity leak out spectroscopy (CALOS) as described in detail below.[11]

Detection of nitric oxide

Three methods were used for detection of NO. In one series of experiments, the release of gaseous NO from skin and skin specimens was collected in an oxygen-free chamber and quantified using the chemiluminescence detector (CLD 77 Amsp) from Eco Physics (Ann Arbor, MI, USA). In a second series of experiments, *in-vivo* release of NO in the skin tissue was determined by *in-vivo* NO-spin trapping with iron-diethylthiocarbamate (Fe-DETC) complexes. Upon trapping of NO, these complexes form a paramagnetic mononitrosyl-iron complex (MNIC). The yield of MNIC in skin biopsies was quantified using electron paramagnetic resonance spectroscopy (EPR). In the third series ^{15}NO was detected by cavity leak out spectroscopy (CALOS).

Quantification of nitrite and nitroso compounds by CLD

The concentrations of nitrite and nitrosated compounds (RX-NO) or S-nitrosothiols (RS-NO) in blood and dermal tissue were quantified by reductive denitrosation of plasma or of skin homogenate supernatant samples using a mixture of iodine/iodide in glacial acetic acid and subsequent detection of the liberated NO by its gas-phase chemiluminescence reaction with ozone, essentially as described.[12] Nitrite concentrations were determined by the difference in peak areas of untreated aliquots and those subjected to preincubation with 0.5% sulfanilamide/HCl, the latter representing total nitrosated species.[13] Discrimination between S-nitrosated molecules (RS-NO) and other nitroso species was achieved by preincubation of sample aliquots with mercuric chloride ($HgCl_2$; 0.2%), which selectively cleaves S-NO

bonds while preserving N-nitroso moieties, followed by sulfanilamide.[12] The chemiluminescence detector was calibrated weekly using a 100 ppb mixture of NO in N_2 or He and calculated NO amounts were validated by injection of freshly prepared nitrite standards into the reaction mixture.

Alternatively, nitrite and RS-NO was determined in culture supernatants using the diazotisation reaction as modified by Wood et al. [14] and $NaNO_2$ as standard.

EPR spectroscopy

Fresh skin specimens were kept in DMEM medium at pH 7.4 and 37°C under a controlled atmosphere containing 20 % O_2, 5 % CO_2 and 75 % N_2. Within 1 hr of surgery, the small 1cm x 1cm section of skin were loaded with Fe-DETC complexes for NO trapping. Such complexes are hydrophobic [15, 16] and were produced *in situ* in the low polarity compartments (lipid and protein) of the skin by two successive soaking steps taking a total of 1 hr. In the first, iron was loaded by soaking for 30 min in DMEM containing 150 μM iron-citrate. After rinsing with fresh DMEM to remove free iron-citrate, the skin was soaked for 30 min in DMEM containing 300 μM diethyldithiocarbamate (DETC) ligands. After ca 15 min exposure to DETC, the inner dermal side of the skin showed a noticeable dark-pink hue indicating formation of the strongly absorbing dark Fe^{3+}-DETC complexes in the tissue. Visual inspection of a tissue cross section confirmed that the dark-pink hue was not restricted to the outer dermal surface but extended into the interior tissue. It was verified by visual and microscopic inspection that formation of black particulates (solid insoluble Fe^{3+}-DETC crystals) did not occur in the medium. After loading with DETC ligands, the skin sections were again rinsed with fresh medium prior to the start of the actual trapping experiment. Placing the skin sections on ice terminated the trapping experiments. Small (ca. 200 – 250 mg) sections were cut, immersed in strong HEPES buffer (150 mM, pH 7.4) and snap frozen in liquid nitrogen until EPR assay. In order to discriminate NO formation in different skin thicknesses, specimens were split in

horizontal sections of 1.0 - 1.5 mm by a razor blade and sections were treated exactly as described above. In some experiments, enzymatic NO production was inhibited by administration of 1 mM L-NIO. In this case, the L-NIO was present during the 30 min incubation with DETC ligand, as well as during the actual trapping experiment. Alternatively, in some experiments the apical side of this skin section had been treated with cream containing ^{15}N-Nitrite (5 mM) prior to UVA. After numerical subtraction of an experimental spectrum of ^{15}NO-Hb, the difference spectrum was calculated

The incubation times for the trapping experiments were calculated from the time point when loading with Fe-DETC was completed. We note that some formation of MNIC adducts may already occur during the incubation with DETC ligands since Fe-DETC traps are formed as soon as the iron-loaded skin is brought into contact with DETC. The quantity of these preformed MNIC adducts in Fe-DETC loaded skin sections remained below the EPR detection limit of ca 30 pmol MNIC, and was neglected. The EPR spectra were measured at 77 K on a modified X-band ESP300 spectrometer (Bruker BioSpin, Rheinstetten, Germany) operating with 20 mW microwave power. The skin specimens weighed ca 200 - 250 mg, and were immersed in strong HEPES buffer (150 mM, pH 7.4) and snap frozen in liquid nitrogen as small frozen columns of 4.8 mm diameter and a volume of ca 400 ± 20 µl. These columns were placed at the bottom of a quartz liquid finger dewar filled with liquid nitrogen. The sample was carefully centered inside a Bruker ER4103TM cylindrical cavity operating in TM_{110} mode with unloaded Q ~ 10.000. The magnetic field was modulated at a frequency of 100 kHz with 5 G amplitude. The detector gain was $2 \cdot 10^5$, time constant 82 ms, and ADC conversion time 82 ms. Up to four field sweeps were accumulated to improve signal to noise. With these spectrometer settings, the detection limit was ca 30 pmol MNIC. The MNIC yields in the tissue samples were quantified by comparison with frozen reference samples of paramagnetic NO-Fe^{2+}-MGD complexes (10 µM) in PBS buffer. The absolute

accuracy of the MNIC yields is better than10 %.

NO spin trapping is widely used in biological systems and formation of paramagnetic MNIC adducts is usually taken as evidence for free NO radicals. This is not strictly true, since S-nitrosothiols may also transfer the NO moiety to Fe-dithiocarbamate traps in a direct trans-nitrosylation reaction. However, the reaction rate is 6 orders of magnitude smaller than the trapping rate of free NO radicals,[17] and makes this alternative pathway of MNIC formation negligible in biological systems.

Detection of ^{15}NO by cavity leak out spectroscopy

The cavity leak out spectroscopy (CALOS) set-up has been developed mainly for trace gas analysis in atmospheric and medical applications.[18] The method is based on laser absorption spectroscopy, which utilizes the fact that molecules absorb light at distinct frequencies. For NO, the strongest absorption features are located in the mid-infrared wavelength region near 5 µm. Due to well separated vibronic absorption lines even differentiation of different isotopologues of NO is possible. We used a CO sideband laser operating at 5.26 µm (1900 cm^{-1}) and 5.30 µm (1874 cm^{-1}) for ^{14}NO and ^{15}NO detection, respectively, providing a sideband power of about 120 µW. The laser light is coupled into a high finesse cavity consisting of two high reflective mirrors (R >99.99%), which is used as absorption cell. The transmitted laser power (2.5% of the incident power) is detected by a LN_2-cooled InSb photodector (3.5 A/W at 1875 cm^{-1}).

The resulting effective absorption path length (>5 km), which can roughly be estimated by dividing the cavity length (0.5 m) by the mirror transmission, allows the determination of extremely low absorption coefficients. The noise-equivalent absorption coefficient is 1.2×10^{-10} cm^{-1} at an integration time of 100 s, corresponding to 18 ppt ^{14}NO and 16 ppt ^{15}NO. Shorter integration times lead to slightly lower sensitivity. The time resolution is limited by the gas exchange time of the absorption cell which is less than 800 ms.[19]

Statistical analysis

Values were reported as mean ± standard deviations (SD). For statistical analysis we used ANOVA followed by an appropriate post-hoc multiple comparison test (Tukey method). A $p<0.05$ was considered significant.

REFERENCES

1. Berardesca E, Maibach H. Racial differences in skin pathophysiology. *J Am Acad Dermatol.* 1996;34(4):667-672.
2. Suschek CV, Bruch-Gerharz D, Kleinert H, Förstermann U, Kolb-Bachofen V. Ultraviolet A1 radiation induces nitric oxide synthase-2 expression in human skin endothelial cells in the absence of proinflamatory cytokines. *J. Invest. Dermatol.* 2001;117:1200-1205.
3. Suschek CV, Paunel A, Kolb-Bachofen V. Nonenzymatic nitric oxide formation during UVA irradiation of human skin: experimental setups and ways to measure. *Methods Enzymol.* 2005;396:568-578.
4. Paunel AN, Dejam A, Thelen S, Kirsch M, Horstjann M, Gharini P, Murtz M, Kelm M, de Groot H, Kolb-Bachofen V, Suschek CV. Enzyme-independent nitric oxide formation during UVA challenge of human skin: characterization, molecular sources, and mechanisms. *Free Radic Biol Med.* 2005;38(5):606-615.
5. Mnaimneh S, Geffard M, Veyret B, Vincendeau P. Albumin nitrosylated by activated macrophages possesses antiparasitic effects neutralized by anti-NO-acetylated-cysteine antibodies. *J Immunol.* 1997;158(1):308-314.
6. Mnaimneh S, Geffard M, Veyret B, Vincendeau P. Detection of nitrosylated epitopes in Trypanosoma brucei gambiense by polyclonal and monoclonal anti-conjugated-NO-cysteine antibodies. *C R Acad Sci III.* 1999;322(4):311-322.
7. Kelm M, Preik M, Hafner DJ, Strauer BE. Evidence for a multifactorial process involved in the impaired flow response to nitric oxide in hypertensive patients with endothelial dysfunction. *Hypertension.* 1996;27(3 Pt 1):346-353.
8. Preik M, Lauer T, Heiss C, Tabery S, Strauer BE, Kelm M. Automated ultrasonic measurement of human arteries for the determination of endothelial function. *Ultraschall Med.* 2000;21(5):195-198.
9. Ishii K, Sheng H, Warner TD, Forstermann U, Murad F. A simple and sensitive bioassay method for detection of EDRF with RFL-6 rat lung fibroblasts. *Am J Physiol.* 1991;261(2 Pt 2):H598-603.
10. Grisham MB, Johnson GG, Lancaster JR. Quantitation of nitrate and nitrite in extracellular fluids. *Nitric Oxide, Pt a - Sources and Detection of No; No Synthase.* 1996;268:237-246.
11. Fritsch T, Brouzos P, Heinrich K, Kelm M, Rassaf T, Hering P, Kleinbongard P, Murtz M. NO detection in biological samples: differentiation of 14 NO and 15 NO using infrared laser spectroscopy. *Nitric Oxide.* 2008;19(1):50-56.
12. Feelisch M, Rassaf T, Mnaimneh S, Singh N, Bryan NS, Jourd'Heuil D, Kelm M. Concomitant S-, N-, and heme-nitros(yl)ation in biological tissues and fluids: implications for the fate of NO in vivo. *Faseb J.* 2002;16(13):1775-1785.
13. Marley R, Feelisch M, Holt S, Moore K. A chemiluminescense-based assay for S-nitrosoalbumin and other plasma S-nitrosothiols. *Free Radic Res.* 2000;32(1):1-9.
14. Wood KS, Buga GM, Byrns RE, Ignarro LJ. Vascular smooth muscle-derived relaxing factor (MDRF) and its close similarity to nitric oxide. *Biochem. Biophys. Res. Commun.* 1990;170:80-87.

15. van Faassen EE, Koeners MP, Joles JA, Vanin AF. Detection of basal NO production in rat tissues using iron-dithiocarbamate complexes. *Nitric Oxide-Biology and Chemistry.* 2008;18(4):279-286.
16. Vanin AF, Bevers LM, Mikoyan VD, Poltorakov AP, Kubrina LN, van Faassen E. Reduction enhances yields of nitric oxide trapping by iron-diethyldithiocarbamate complex in biological systems. *Nitric Oxide-Biology and Chemistry.* 2007;16(1):71-81.
17. van Faassen EE, Vanin AF. Mononitrosyl-iron complexes with dithiocarbamate ligands: physico-chemical properties. In: van Faassen EE, Vanin AF, eds. *Radicals for life: The various forms of nitric oxide.* Amsterdam: Elsevier; 2007:383-388.
18. Murtz M, Frech B, Urban W. High-resolution cavity leak-out absorption spectroscopy in the 10-mu m region. *Applied Physics B-Lasers and Optics.* 1999;68(2):243-249.
19. Halmer D, von Basum G, Horstjann M, Hering P, Murtz M. Time resolved simultaneous detection of 14NO and 15NO via mid-infrared cavity leak-out spectroscopy. *Isotopes Environ Health Stud.* 2005;41(4):303-311.